Supplement of Atmos. Chem. Phys., 21, 13369–13395, 2021
https://doi.org/10.5194/acp-21-13369-2021-supplement

Atmospheric Chemistry and Physics
Open Access
EGU

Supplement of

Global dust optical depth climatology derived from CALIOP and MODIS aerosol retrievals on decadal timescales: regional and interannual variability

Qianqian Song et al.

Correspondence to: Zhibo Zhang (zhibo.zhang@umbc.edu)

DAOD derived from CALIOP and MODIS observations

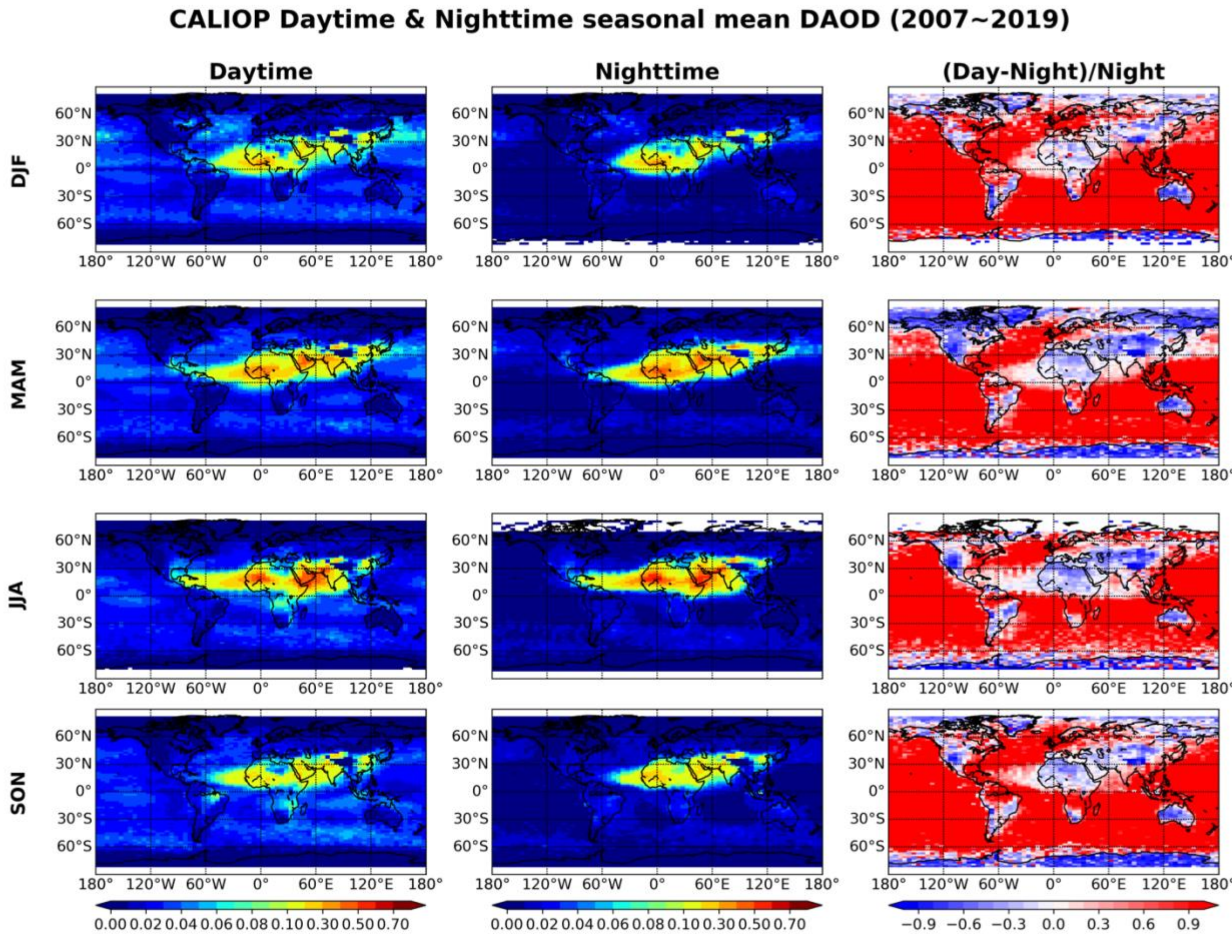

Figure S1 Seasonal mean DAOD derived from CALIOP daytime (column 1) and nighttime (column 2) observations. Column 3 indicates the difference of daytime and nighttime DAOD, which is expressed as $\frac{DAOD_{daytime} - DAOD_{nighttime}}{DAOD_{nighttime}}$

Table S1. Summary of Quality Assurance procedures in CALIOP- and MODIS-based DAOD retrievals.

	Quality Assurance (references)
CALIOP	(a) Select cloud-free columns or columns with high-level optically thin clouds using CALIOP L2 cloud layer product. (Yu et al. 2015a) (b) Use CAD score between –90 and –100 (Yu et al. 2019) (c) Use EXT_QC values of 0, 1, 18, and 16 (Winker et al. 2013)
MODIS (Ocean)	QAC>=0 (Levy et al. 2013), AOD <0 was excluded
MODIS (Land)	Retrieved aerosol properties with a standard deviation less than 0.15 among 10x10 pixels are assumed cloud free and are flagged with the highest quality flag (QA=3). Here we use products of QA=3 following the recommendation of Hsu et al. (2013)

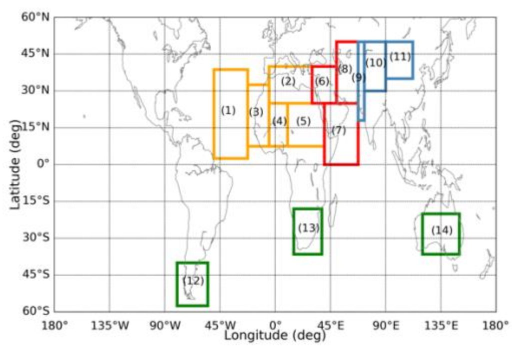

Figure S2. Region definition based on Ridley et al. 2016.

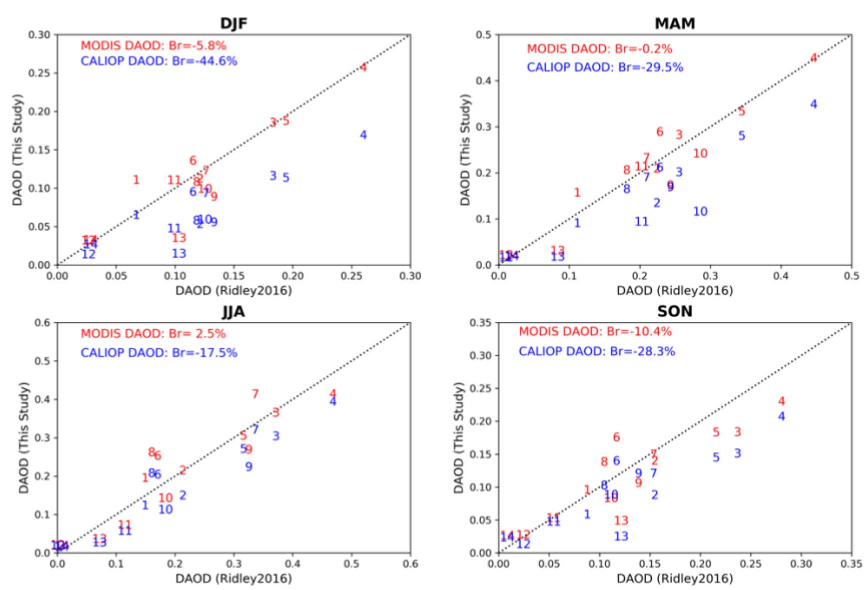

Figure S3. Compare seasonal mean DAOD (2004~2008) from Ridley et al. 2016 with our (2007~2019) seasonal mean DAOD based on CALIOP (blue markers) and MODIS (red markers) for each region. Each number in this plot represent the corresponding regions indicated in Figure S2. $B_r^{Modis} = \overline{DAOD}_{Modis} / \overline{DAOD}_{Ridley} - 1$, $B_r^{Caliop} =$

$\overline{DAOD}_{Caliop} / \overline{DAOD}_{Ridley} - 1$. The specific values of seasonal mean DAOD from MODIS and CALIOP retrievals for the 14 regions are shown in Table S2.

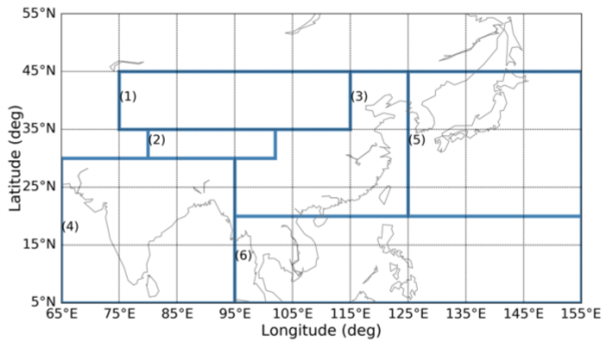

Figure S4. Region definition based on Proestakis et al. 2018.

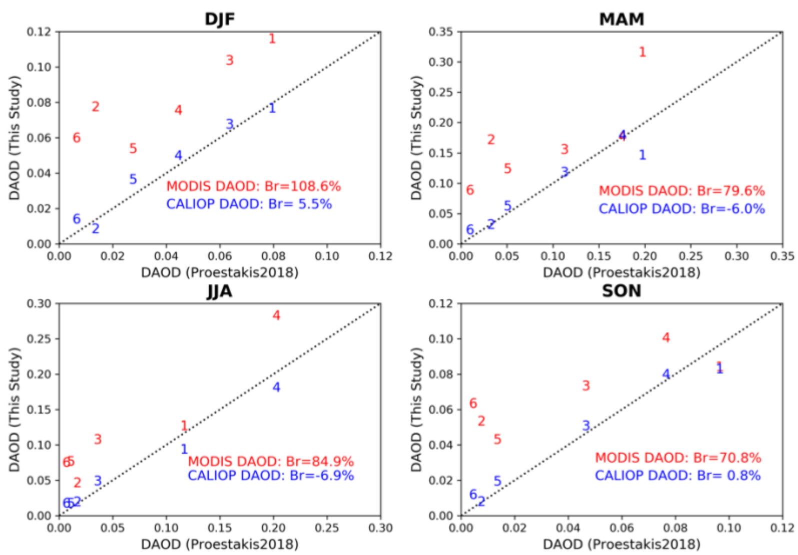

Figure S5. Compare seasonal mean DAOD (2007~2015) from Proestakis et al. 2018 with our seasonal mean DAOD (2007~2015) based on CALIOP (blue markers) and MODIS (red markers). Each number in the plot represent the corresponding regions in Figure S4. $B_r^{Modis} = \overline{DAOD}_{Modis} / \overline{DAOD}_{Proestakis} - 1$, $B_r^{Caliop} = \overline{DAOD}_{Caliop} / \overline{DAOD}_{Proestakis} - 1$. The specific values of seasonal mean DAOD from MODIS and CALIOP retrievals for the 6 regions are shown in Table S3.

Table S2. MODIS-based and CALIOP-based DAOD for regions indicated in Figure S2.

Region	Latitude Longitude	DJF		MAM		JJA		SON	
		MODIS	CALIOP	MODIS	CALIOP	MODIS	CALIOP	MODIS	CALIOP
(1)	(2.5, 38.75) (–50, –22.5)	0.106	0.060	0.148	0.082	0.185	0.114	0.090	0.053
(2)	(25, 40) (–5, 30)	0.107	0.048	0.200	0.126	0.204	0.140	0.134	0.082
(3)	(7.5, 32.5) (–22.5, –5)	0.180	0.111	0.274	0.192	0.355	0.294	0.177	0.145
(4)	(7.5, 25) (–5, 10)	0.252	0.164	0.441	0.340	0.404	0.384	0.224	0.201
(5)	(7.5, 25) (10, 40)	0.183	0.109	0.325	0.272	0.295	0.261	0.177	0.139
(6)	(25, 40) (30, 50)	0.130	0.090	0.280	0.203	0.242	0.193	0.169	0.134
(7)	(0, 25) (40, 67.5)	0.118	0.088	0.224	0.182	0.403	0.311	0.144	0.115
(8)	(25, 50) (50, 67.5)	0.103	0.053	0.197	0.156	0.252	0.197	0.132	0.096
(9)	(18, 50) (67.5, 72.5)	0.084	0.051	0.164	0.160	0.258	0.213	0.100	0.115
(10)	(30, 50) (72.5, 90)	0.094	0.054	0.233	0.107	0.132	0.102	0.077	0.082
(11)	(35, 50) (90, 112)	0.105	0.043	0.205	0.085	0.062	0.047	0.047	0.042
(12)	(–57.5, –40) (–80, –55)	0.027	0.009	0.013	0.008	0.011	0.009	0.022	0.007
(13)	(–36.5, –18) (15, 38)	0.030	0.009	0.022	0.009	0.026	0.017	0.043	0.019
(14)	(–36.5, –20) (120, 150)	0.028	0.021	0.012	0.010	0.009	0.006	0.020	0.018

Table S3. MODIS-based and CALIOP-based DAOD for regions indicated in Figure S4.

Region	(Latitude)(Longitude)	DJF		MAM		JJA		SON	
		MODIS	CALIOP	MODIS	CALIOP	MODIS	CALIOP	MODIS	CALIOP
(1)	(35, 45) (70, 115)	0.113	0.074	0.309	0.139	0.121	0.088	0.082	0.080
(2)	(30, 35) (80, 102)	0.075	0.006	0.164	0.025	0.040	0.013	0.051	0.005
(3)	(35, 45) (115, 125) (30, 35) (102,125) (20,30) (95,125)	0.101	0.065	0.148	0.111	0.101	0.043	0.071	0.048
(4)	(5, 30) (65, 95)	0.073	0.048	0.170	0.172	0.277	0.175	0.098	0.077
(5)	(20,45) (125, 155)	0.051	0.034	0.117	0.056	0.071	0.012	0.041	0.017
(6)	(5, 20) (95, 155)	0.057	0.012	0.081	0.016	0.069	0.011	0.061	0.009

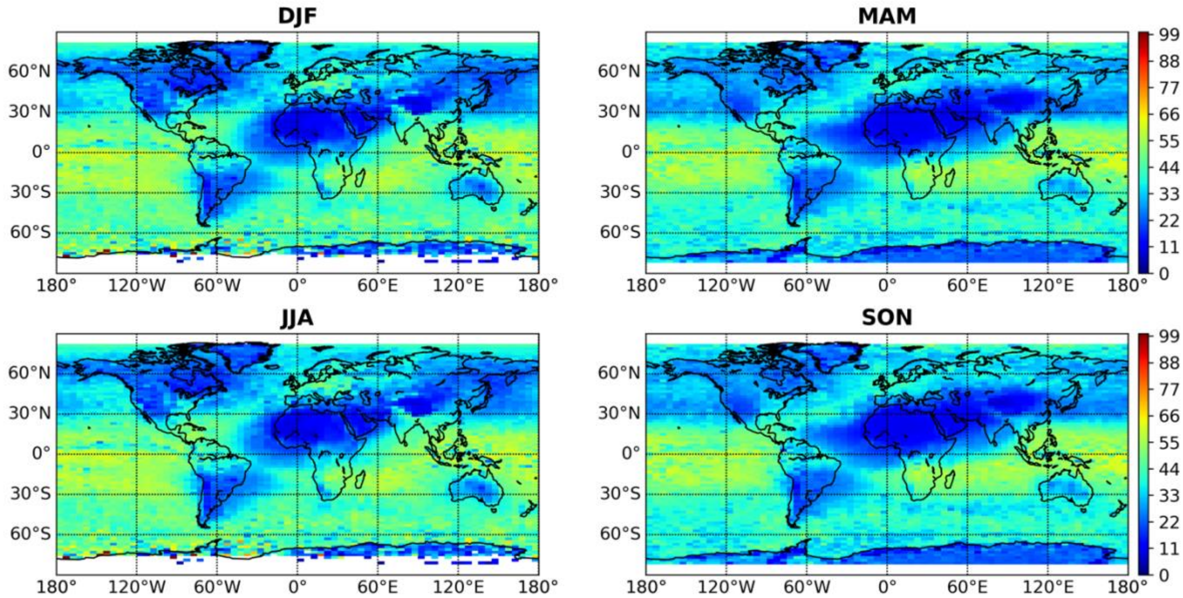

Figure S6. 2007~2019 Seasonal mean DAOD uncertainties induced by DPR assumptions. For each season in each grid, DAOD uncertainty is defined as $\frac{(DAOD^{high} - DAOD^{low})/2}{DAOD^{mean}}\%$, where $DAOD^{high}$ is derived from high dust scenario with $\delta_d = 0.20$ and $\delta_{nd} = 0.02$, $DAOD^{low}$ is derived from low dust scenario with $\delta_d = 0.30$ and $\delta_{nd} = 0.07$, $DAOD^{mean}$ is the average of the two scenarios.

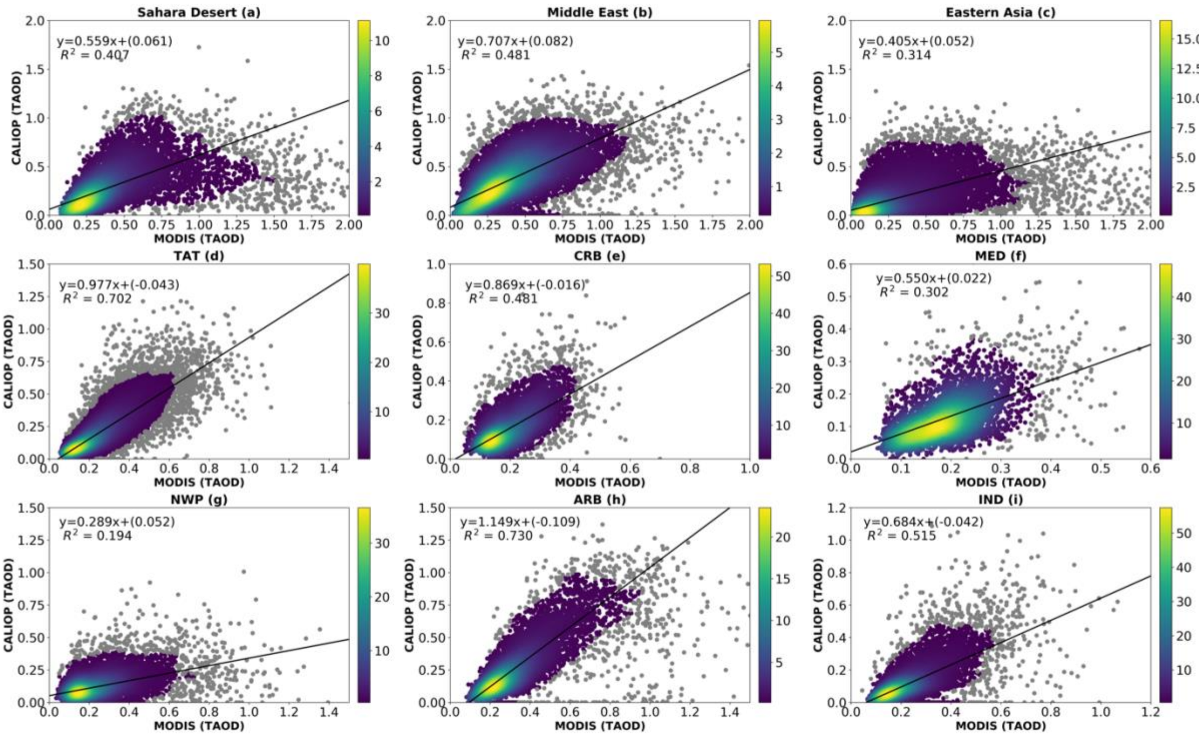

Figure S7. Comparison of CALIOP TAOD against MODIS TAOD over dust-laden regions indicated in Figure 8. Color represents the probability density using gaussian kernel density estimation. Grey points represent data points within the lowest 5% of data density. Those grey points are excluded in the linear regression analysis.

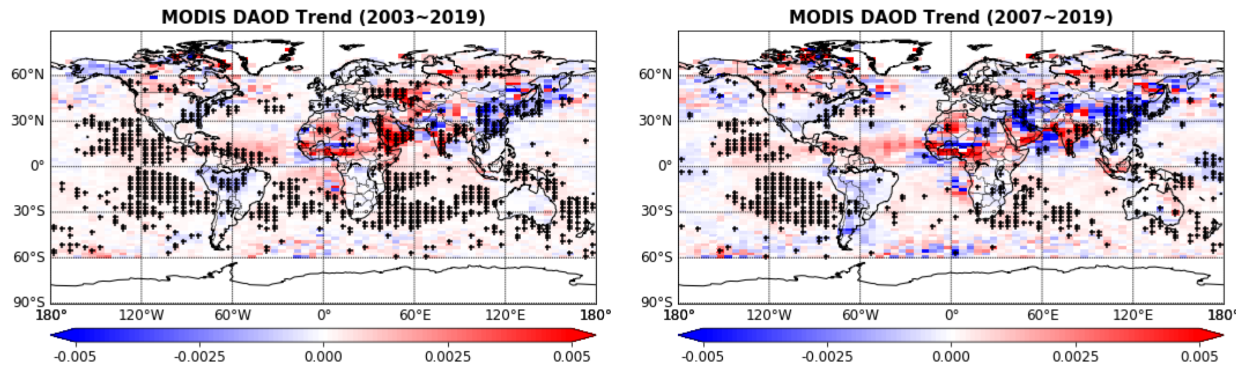

Figure S8. Same as Figure 14, except for TAOD.

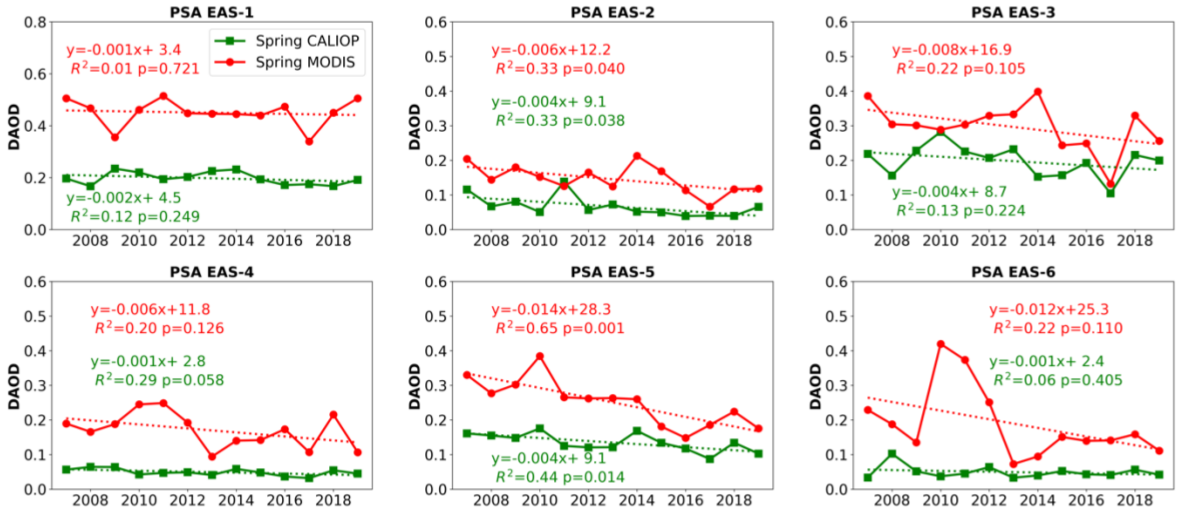

Figure S9. Same as Figure 16, except for inter-spring variability.

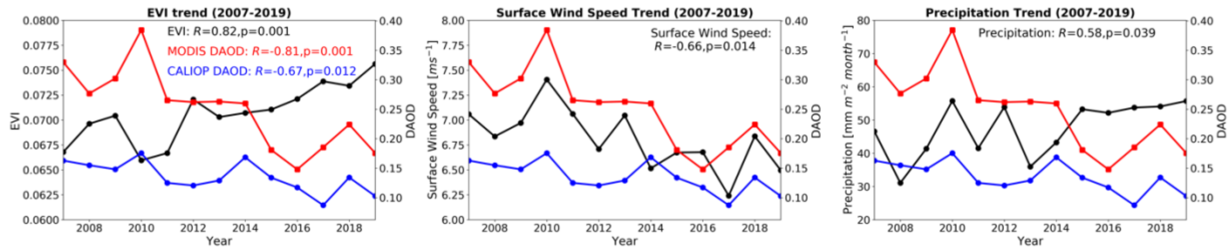

Figure S10. Inter-spring series of EVI, surface wind speed and precipitation along with inter-spring series of DAOD from MODIS (red curves) and CALIOP (blue curves). R is Pearson's linear correlation coefficient between each variables and time series. Positive R indicates the variable increase with time, and vice versa.

Comparison with previous studies

Our MODIS DAOD study and Voss and Evan 2020 use the similar method to derive DAOD. However, there is a subtle difference in our MODIS over ocean retrieval methodology, which is the main reason causing the non-negligible difference in our over-ocean mean DAOD. We use MODIS over ocean retrievals to determine $f_c, f_{d,} f_m$, while Voss and Evan 2020 determine those parameters based on AERONET stations dominated by each aerosol type. $f_c, f_{d,} f_m$ used in those two studies are shown in Table S4.

Based on Eq. (2) and (3) in the paper, we derived the relationship of DAOD (τ_d) with each of parameters ($f_c, f_{d,} f_m$):

$$\tau_d = \frac{(\tau - \tau_m)f_c + \tau_m f_m - \tau f}{f_c - f_d}$$

Then, the change of τ_d with respect to each of the three parameters $f_c, f_{d,} f_m$ are expressed as:

$\frac{\partial \tau_d}{\partial f_c} = \frac{\tau_c}{(f_c - f_d)}$, $\frac{\partial \tau_d}{\partial f_d} = \frac{\tau_d}{(f_c - f_d)}$, $\frac{\partial \tau_d}{\partial f_m} = \frac{\tau_m}{(f_c - f_d)}$. Based on Table S4, f_c is much larger than f_d in both studies, so that $(f_c - f_d) > 0$. In addition, τ_c, τ_d and τ_m are always larger than zero. Therefore, we have $\frac{\partial \tau_d}{\partial f_c} > 0$, $\frac{\partial \tau_d}{\partial f_d} > 0$, $\frac{\partial \tau_d}{\partial f_m} > 0$. This means that τ_d is positively proportional to $f_c, f_{d,} f_m$, respectively. In other words, τ_d increases as each of those parameters increasing.

Table S4. $f_c, f_{d,} f_m$ used in over-ocean Aqua MODIS Collection 6 DAOD retrieval and in Voss and Evan 2020. The last column shows the relationship of each parameter with the retrieved DAOD, '+' means DAOD increases as the parameter increasing, '–' means DAOD decreases as the parameter increasing.

	Aqua MODIS C6	Voss and Evan 2020	Relation with τ_d
f_c	0.89	0.79	+
f_d	0.31	0.35	+
f_m	0.48	0.34	+

It turns out that we used significantly larger f_c and f_m, while a slightly smaller f_d, in comparison with VE20. Because the derived DAOD is positively proportional to these parameters, the use of larger f_c and f_m, is probably the reason for a larger DAOD in our study.